STEM CELLS TRANSLATIONAL MEDICINE®

STANDARDS, PROTOCOLS, POLICIES, AND REGULATIONS FOR CELL-BASED THERAPIES

Role of Human-Induced Pluripotent Stem Cell-Derived Spinal Cord Astrocytes in the Functional Maturation of Motor Neurons in a Multielectrode Array System

ARENS TAGA,[a] RAHA DASTGHEYB,[a] CHRISTA HABELA,[a] JESSICA JOSEPH,[a] JEAN-PHILIPPE RICHARD,[a] SARAH K. GROSS,[a] GIUSEPPE LAURIA,[b,c] GABSANG LEE,[a,d] NORMAN HAUGHEY,[a] NICHOLAS J. MARAGAKIS[a]

Key Words. Electrophysiology • Spinal cord • Glutamate receptor • Gap junction • Glia

[a]Department of Neurology, Johns Hopkins University, Baltimore, Maryland, USA; [b]Fondazione I.R.C.C.S. Istituto Neurologico Carlo Besta, Milan, Italy; [c]Department of Biomedical and Clinical Sciences "Luigi Sacco", University of Milan, Milan, Italy; [d]Department of Neuroscience, Johns Hopkins University, Baltimore, Maryland, USA

Correspondence: Nicholas J. Maragakis, M.D., Department of Neurology, Johns Hopkins University, The John G. Rangos Sr. Bldg. 855 North Wolfe Street, Room 248, 2nd Floor, Baltimore, Maryland 21205, USA. Telephone: 1-410-614-9874; e-mail: nmaragak@jhmi.edu

Received May 16, 2019; accepted for publication August 30, 2019; first published October 21, 2019.

http://dx.doi.org/10.1002/sctm.19-0147

ABSTRACT

The ability to generate human-induced pluripotent stem cell (hiPSC)-derived neural cells displaying region-specific phenotypes is of particular interest for modeling central nervous system biology in vitro. We describe a unique method by which spinal cord hiPSC-derived astrocytes (hiPSC-A) are cultured with spinal cord hiPSC-derived motor neurons (hiPSC-MN) in a multielectrode array (MEA) system to record electrophysiological activity over time. We show that hiPSC-A enhance hiPSC-MN electrophysiological maturation in a time-dependent fashion. The sequence of plating, density, and age in which hiPSC-A are cocultured with MN, but not their respective hiPSC line origin, are factors that influence neuronal electrophysiology. When compared to coculture with mouse primary spinal cord astrocytes, we observe an earlier and more robust electrophysiological maturation in the fully human cultures, suggesting that the human origin is relevant to the recapitulation of astrocyte/motor neuron crosstalk. Finally, we test pharmacological compounds on our MEA platform and observe changes in electrophysiological activity, which confirm hiPSC-MN maturation. These findings are supported by immunocytochemistry and real-time PCR studies in parallel cultures demonstrating human astrocyte mediated changes in the structural maturation and protein expression profiles of the neurons. Interestingly, this relationship is reciprocal and coculture with neurons influences astrocyte maturation as well. Taken together, these data indicate that in a human in vitro spinal cord culture system, astrocytes support hiPSC-MN maturation in a time-dependent and species-specific manner and suggest a closer approximation of in vivo conditions. STEM CELLS TRANSLATIONAL MEDICINE *2019;8:1272–1285*

SIGNIFICANCE STATEMENT

This study develops a method by which human-induced pluripotent stem cell-derived astrocytes (hiPSC-A) with distinct spinal cord identity are cocultured with spinal cord motor neurons (hiPSC-MN) for multielectrode array (MEA) recordings. It also demonstrates that hiPSC-A influence the morphological, molecular, and electrophysiological maturation of hiPSC-MN. Similarly, this study shows that hiPSC-A maturation is enhanced by the coculture with hiPSC-MN. This fully human, spinal cord-specific, coculture platform with MEA analyses provides a new tool for investigating astrocyte/MN interactions and has the potential to more accurately model human diseases with spinal cord pathology, including spinal muscular atrophy and amyotrophic lateral sclerosis.

INTRODUCTION

Human-induced pluripotent stem cell-derived neurons (hiPSC-N) and astrocytes (hiPSC-A) provide a powerful platform to recapitulate central nervous system biology in vitro in both normal and disease states and to explore therapeutic strategies for neurological disorders [1]. With the increasing number of differentiation techniques, the electrophysiological characterization of hiPSC-N has become crucial to provide accurate measures of their function, beyond morphological studies, and, ideally, within an environment that resembles their in vivo counterparts.

Multielectrode arrays (MEA) are particularly suited for these purposes [2] as they enable the recording of large populations of neurons and their network activity, and have the potential to inform about neuron–glia interactions. This is achieved through the detection of extracellular voltages, which reflect the spike activity of local neuronal populations. The extracellular nature of the recordings allows for extended recordings that are particularly suitable for drug testing.

Previous MEA studies have focused on hiPSC-derived cortical neurons, either alone [3–5] or in coculture with primary rodent cortical astrocytes [6] and more recently with hiPSC-derived astrocytes [4, 7–9]. Despite an established body of evidence suggesting that astrocytes contribute to neuronal electrophysiological maturation by promoting synaptogenesis [10], MEA- and hiPSC-based paradigms, still influenced by a traditionally neuron-centered perspective, have not yet been used to model this unique glial contribution. Well-established literature [11, 12] has suggested that astrocytes are regionally heterogeneous and that astrocyte–neuron interactions may be influenced by their positional identities. However, hiPSC-A have been largely used as a homogenous and interchangeable cell type for MEA- and iPSC-based studies.

We describe, for the first time, a method in which the coculture of spinal cord hiPSC-A and hiPSC-derived spinal cord motor neurons (hiPSC-MN) is optimized for obtaining MEA electrophysiological recordings. We use this platform to examine the bidirectional interactions between hiPSC-A and hiPSC-MN and to investigate glial contribution to the electrophysiological maturation of hiPSC-MN.

Materials and Methods

Generation of hiPSC, hiPSC-MN, and hiPSC-A

hiPSCs were generated using a four-vector method as we have previously described [13]. For this study, we used three different cell lines from healthy subjects: CIPS, GM01582, and CS25. We used previously described protocols to differentiate hiPSC-MN [14, 15] and hiPSC-A [15] with spinal cord regional identity (Fig. 1A), as indicated by the expression of region-specific markers, that is, choline acetyltransferase (ChAT) [14] and HOXB4 [15], respectively (Fig. 1A′, 1A″).

MEA Culture

Unless stated otherwise, for cultures on MEA plates (60MEA200/30iR-Ti-gr, multichannel systems; MCS; Fig. 1B), we used hiPSC-MN derived from the GM01582 cell line and hiPSC-A derived from the CIPS cell line. For hiPSC-MN monocultures, neurons were plated after 60DIV at a density of 5×10^5 cells per plate; this neuron density was maintained as a constant for all culture conditions. For hiPSC-A monocultures, astrocytes were plated after 90DIV at a density of 1×10^5 cells per plate. For the "astrocyte first" serial coculture, we first plated hiPSC-A cultured for 86DIV at a density of 1×10^5 cells per plate; 4 days later, we added hiPSC-MN cultured for 60DIV. For the "neuron first" serial coculture, we first plated hiPSC-MN cultured for 56DIV; 4 days later, we added hiPSC-A cultured for 90DIV and then plated at a density of 1×10^5 cells per plate. For the simultaneous coculture of hiPSC-A/hiPSC-MN, both cell types were mixed and plated simultaneously on MEA plates at the densities noted above, after 90DIV and 60DIV, respectively (Fig. 1C).

As variations of the above-mentioned simultaneous coculture, we also used the following: hiPSC-A which had been cultured for 60DIV ("immature hiPSC-A") instead of 90DIV, a lower density of hiPSC-A (i.e., 0.5×10^5 cells per plate instead of 1×10^5 per plate), and hiPSC-A differentiated from same iPSC line ("isoclonal") as hiPSC-MN (i.e., both lines were GM01582), instead of using different control iPSC lines for astrocytes (CIPS and CS25) and neurons (GM01582; i.e., "heteroclonal"). We also compared isoclonal versus heteroclonal simultaneous cocultures using a different hiPSC-MN line (i.e., CS25). Finally, we used primary mouse spinal cord astrocyte ("mouse A"), instead of human iPSC-A, simultaneously cocultured with hiPSC-MN for some studies.

MEA Recordings

The MEA plates used for this study have 60 electrodes, including 59 active and 1 inactive that represents the reference for unipolar acquisition. All recordings were conducted using an MEA2100 System (MCS) on a stage maintained at 37°C.

The following electrophysiological parameters were analyzed: spike frequency, burst rate, and percentage of spiking and bursting electrodes. Functional connectivity graphs based on spike frequency were generated as recently described [16]. The recording of the baseline activity of MEA plates was performed weekly over a 1-minute period for 4 weeks after plating. Representative raw voltage waveforms, which were used for quantitative analyses are shown in Supporting Information Figure S1.

For pharmacological testing, we recorded baseline MEA activity for 1 minute, activity 1 minute after 100 µl "fresh" medium exchange with the drug vehicle, and 1–10 minutes after the exchange of 100 µl of medium containing the compound of interest and the vehicle.

We tested the following compounds targeting ion channels and/or neurotransmitter receptors, based on the published literature [6]: 100 mM potassium chloride (KCl); 5 µM of the α-amino-3-hydroxy-5-methyl-4-isoxazolepropionic acid (AMPA)/kainate receptor agonist, kainic acid (KA; Abcam, Cambridge, UK); 50 µM of the AMPA/kainite receptor antagonist, cyanquixaline (CNQX; Sigma–Aldrich, St. Louis, MO, USA); 10 µM of the gamma amino butyric acid (GABA) receptor antagonist, bicuculline (Sigma–Aldrich, St. Louis, MO, USA). We also tested compounds targeting glia and verified their effect on neuronal firing; these included: GAP19 (Tocris, Bristol, UK), a connexin 43 hemichannel blocker [17], at concentrations of 34 µM and 340 µM, and dihydrokainic acid (DHK; Tocris, Bristol, UK), an excitatory amino acid 2 (EAAT2) selective blocker, at concentrations of 50 µM and 300 µM [18, 19]. We analyzed the effects of the above-mentioned compounds on 3 MEA plates at two different time points and when at least one electrode showed spike frequency >0: at week 1 or 2 of culture, and at week 3 or 4.

Data Presentation and Statistical Analysis

All data were analyzed using Graph Pad Prism software (La Jolla, CA). Data are presented as bar graphs for mean ± SEM, with individual observations visualized as scatter plot, or as box (interquartile range and median) and whiskers (minimum and maximum). Data were analyzed using one-way analysis of variance, followed by Tukey's test for multiple comparisons and a two-tailed unpaired *t* test, as appropriate.

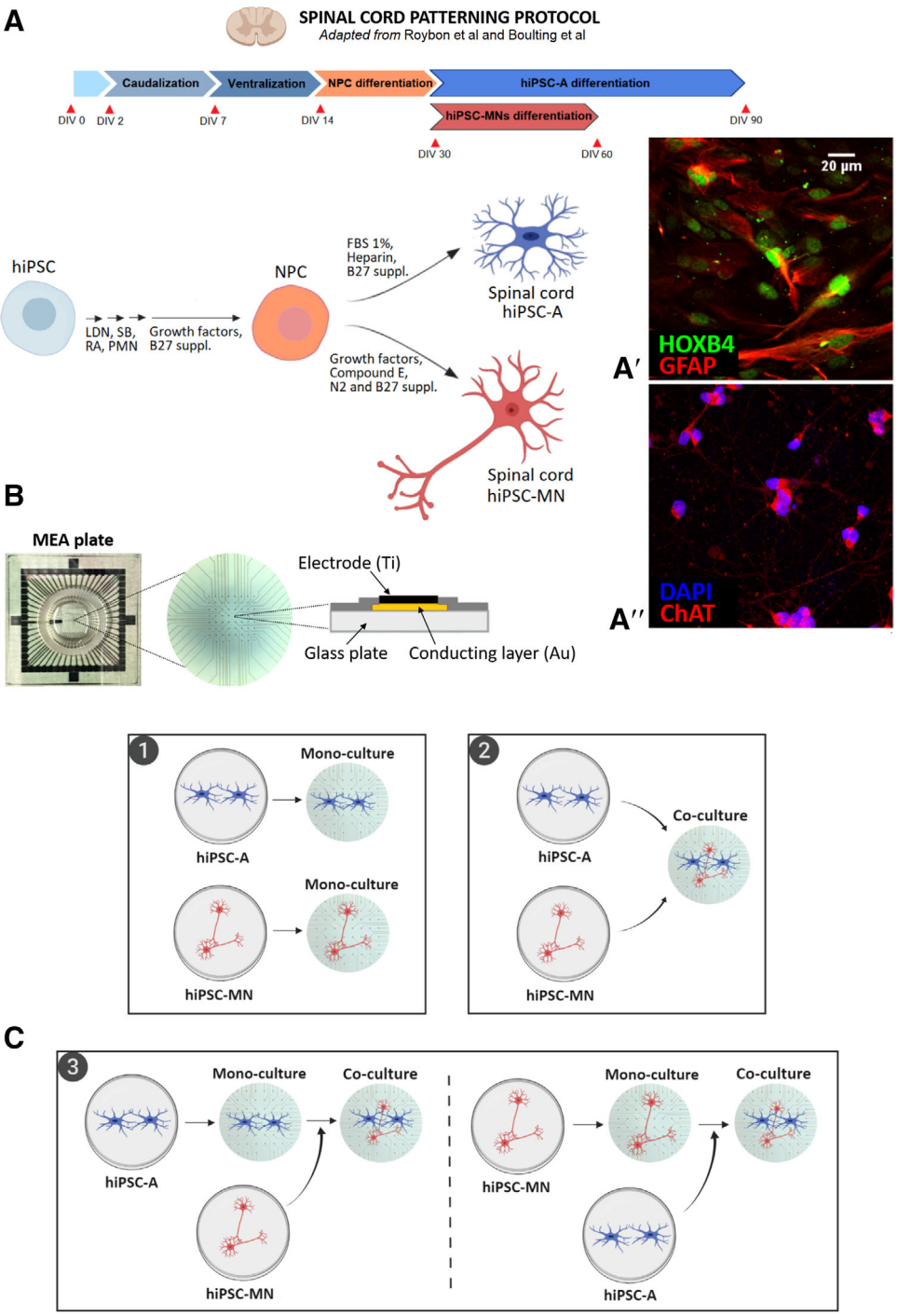

Figure 1. **(A):** Schematic illustration of the differentiation protocol to generate spinal cord human-induced pluripotent stem cell-derived astrocytes (hiPSC-A) and hiPSC-derived motor neurons (hiPSC-MN). Two representative immunofluorescence images of positional identity markers HOXB4 (A′), a transcription factor involved in spinal cord development, and ChAT (A″), an enzyme responsible for the biosynthesis of acetylcholine in spinal cord motor neurons. **(B):** Photograph of multielectrode array (MEA) plate with detail on its set of 60 microelectrodes and schematic illustration of an individual electrode. **(C):** Diagram of hiPSC-A/-MN cultures on MEA plate: **(1)** hiPSC-A or -MN monocultures, where astrocytes or neurons were cultured alone, **(2)** simultaneous coculture, where both cell types were mixed and plated simultaneously, and **(3)** serial cocultures, where hiPSC-A (left) or hiPSC-MN (right) where plated alone prior to the addition of neurons and astrocytes, respectively. Abbreviations: LDN, LDN193189; FBS, fetal bovine serum; RA, retinoic acid; SB, SB431542; PMN, purmorphamine. Illustration created with BioRender.

The statistical significance was set at $p < .05$. Unless stated otherwise, all experiments were performed in technical triplicates.

For qPCR analyses, the ΔΔCT values were normalized to monocultures (i.e., "hiPSC-A" or "hiPSC-MN") to account for the effect of cocultures.

For the analysis of MEA baseline activity, we considered the active electrodes only (i.e., electrodes with spike frequency >0), and their mean activity as a measure of the overall electrophysiological activity of the cell culture. To account for variability in the culturing process, analyses were performed only on parallel plating.

In order to define the effect of KCl and neurotransmitter modulators on MEA activity, we recorded for 3 minutes and compared the mean activity at baseline (1 minute), after medium with vehicle exchange (1 minute) and after drug addition (in the same volume of medium and with the same concentration of vehicle; 1 minute). For GAP19, we recorded for 3 minutes after drug addition, since changes in MEA activity were slightly slower. For DHK, we recorded for 10 minutes after drug addition to detect even slower effects; since changes in the pH in the medium could occur at atmospheric conditions for longer recordings, we compared the activity after DHK addition to parallel plates where we evaluated changes up to 10 minutes after the addition of the vehicle. All experiments were performed in experimental triplicates. Additional methods can be found in Supporting Information.

RESULTS

hiPSC-A Influence hiPSC-MN Maturation

In order to develop a reliable and reproducible platform to study the influences of hiPSC-A on hiPSC-MN electrophysiology, we first sought to optimize the cell culturing protocol on MEA plates, and to determine the optimal sequence of plating hiPSC-A and hiPSC-MN (Supporting Information Fig. S2). Human iPSC-A, after proper treatment of the plate surface and at the densities noted above, generated a confluent monolayer (Supporting Information Fig. S2A, Box 1). The culture of hiPSC-MN alone resulted in large aggregates of neurons, which were arranged over a few electrodes (Supporting Information Fig. S2A, Box 2 and Supporting Information Fig. S2B). The culture of hiPSC-A into a monolayer followed by plating hiPSC-MN resulted in fewer large neuronal aggregates and a more even distribution of cells amongst the electrodes (Supporting Information Fig. S2A, Box 3). Plating hiPSC-MN followed by the addition of hiPSC-A had similar results (not shown). Finally, we found that the simultaneous culture of hiPSC-A and hiPSC-MN resulted in more evenly distributed populations of MN with fewer aggregates of MN and fewer numbers of cells in each aggregate (Supporting Information Fig. S2A, Box 4 and Supporting Information Fig. S2B). These observations were consistent among 15 different MEA cultures.

We then asked whether the presence of astrocytes and the time in culture would result in a change in neuronal subtype composition. When hiPSC-MN were cultured in monocultures for 1 week, we found that >90% of $TUJ1^+$ neurons had a motor neuron identity as demonstrated by ChAT immunoreactivity (Supporting Information Fig. S3A). This percentage was not significantly different when compared with astrocyte–neuron cocultures (93.1% $\pm$ 3.0% vs. 92.1% $\pm$ 4.2%, respectively). This result was confirmed by ISL-1/2 staining of a subset of MN [20], which was between 25% and 30% of $TUJ1^+$ cells for both conditions (28.4% $\pm$ 0.8% vs. 27.4% $\pm$ 1.5%, respectively). Consistent with the spinal cord identity of the neuronal cultures, less than 2% of our neuronal population was positive for CTIP2 (a marker of corticospinal motor neuron identity) [21]. Beside $ChAT^+$ motor neurons, neuronal cultures showed a small proportion (<5%) of GABAergic interneurons, as suggested by the immunoreactivity to GAD67 [22]. These percentages were not influenced by the time in culture, as they were not significantly different after 4 weeks of monoculture or coculture (Supporting Information Fig. S3A), thus reinforcing previous observations that spinal cord motor neuron fate is determined early during hiPSC differentiation [23].

The immunoreactivity for neuronal neurotransmitter receptors (Fig. 2), including AMPA, GABA, and glycine were all significantly increased by the presence of hiPSC-A, both after 1 week (glutamate 2/3 receptor: 7.1% $\pm$ 0.6% vs. 28.9% $\pm$ 0.9%, $p < .001$; GABA receptor: 6.6% $\pm$ 1.1% vs. 16.4% $\pm$ 0.9%, $p < .001$; glycine receptor: 6.2% $\pm$ 1.3% vs. 10.9% $\pm$ 2.0%, $p < .05$) and 4 weeks (glutamate 2/3 receptor: 7.3% $\pm$ 0.4% vs. 28.3% $\pm$ 2.5%, $p < .001$; GABA receptor: 4.8% $\pm$ 1.4% vs. 17.4% $\pm$ 1.9%, $p < .001$; glycine receptor: 5.1% $\pm$ 0.4% vs. 10.2% $\pm$ 1.6%, $p < .05$) of coculture. In parallel to neurotransmitter immunoreactivity, we found that the number of synapses, as demonstrated by PSD95/synaptophysin staining was significantly increased when hiPSC-MN were cocultured with hiPSC-A (Fig. 2). The number of synapses increased over time with the culture of hiPSC-MN alone (6.9 $\pm$ 0.8 vs. 54.2 $\pm$ 8.5, $p < .001$), but to a greater degree (25.5 $\pm$ 2.3 vs. 85.1 $\pm$ 5.1, $p < .01$) in the presence of astrocytes (week 1 monoculture vs. coculture, $p < .01$; week 4 monoculture vs. coculture, $p < .001$; Fig. 2).

We also investigated motor neuron maturation as defined by morphological parameters outlined in Supporting Information Figure S4. First, we considered (n = 100) randomly selected hiPSC-MN neurites in monocultures or cocultures, and found that the mean value of the diameter distribution was significantly different amongst conditions: 1.5 μm $\pm$ 0.6 μm versus 2.1 μm $\pm$ 0.7 μm for week 1 motor neurons in monoculture versus coculture, respectively ($p < .001$), and 2.2 μm $\pm$ 0.6 μm versus 3.0 μm $\pm$ 1.7 μm for week 4 monocultures versus cocultures, respectively ($p < .001$). Notably, after 4 weeks of coculture, a subgroup of larger diameter neurites emerged, as seen in the histogram in Supporting Information Figure S4. We then considered the largest neuronal processes of n = 50 randomly selected neurons, and found that those increased over time, with slightly higher values in the presence of hiPSC-A though not statistically significant: 5.4 μm $\pm$ 1.8 μm versus 9.1 μm $\pm$ 3.1 μm, $p < .001$ for monocultures, and 5.9 μm $\pm$ 2.7 μm versus 9.7 $\pm$ 3.9 μm, $p < .001$ for cocultures. The area of the neuronal cell body (n = 50 neurons) significantly increased over time in hiPSC-MN monocultures (125.9 μm^2 $\pm$ 28.9 μm^2 vs. 203.9 μm^2 $\pm$ 32.6 μm^2, $p < .001$), and more robustly ($p < .001$) in the presence of hiPSC-A (131.1 μm^2 $\pm$ 26.1 μm^2 vs. 230.9 μm^2 $\pm$ 26.3 μm^2, $p < .001$). Finally, to quantify the complexity of connections between neurons we performed a Sholl analysis and found that the mean number of intersections per neuron increased significantly overtime (2.2 $\pm$ 0.3 vs. 14.5 $\pm$ 0.9, $p < .05$), particularly ($p < .001$) when hiPSC-MN where in coculture with hiPSC-A (1.9 $\pm$ 0.2 vs. 38.6 $\pm$ 8.3, $p < .001$).

Through parallel qPCR experiments, we sought to verify our observations from immunostaining and examine the effect of human astrocyte maturity as well as species-specific interactions on neuronal maturation (Supporting Information Fig. S5).

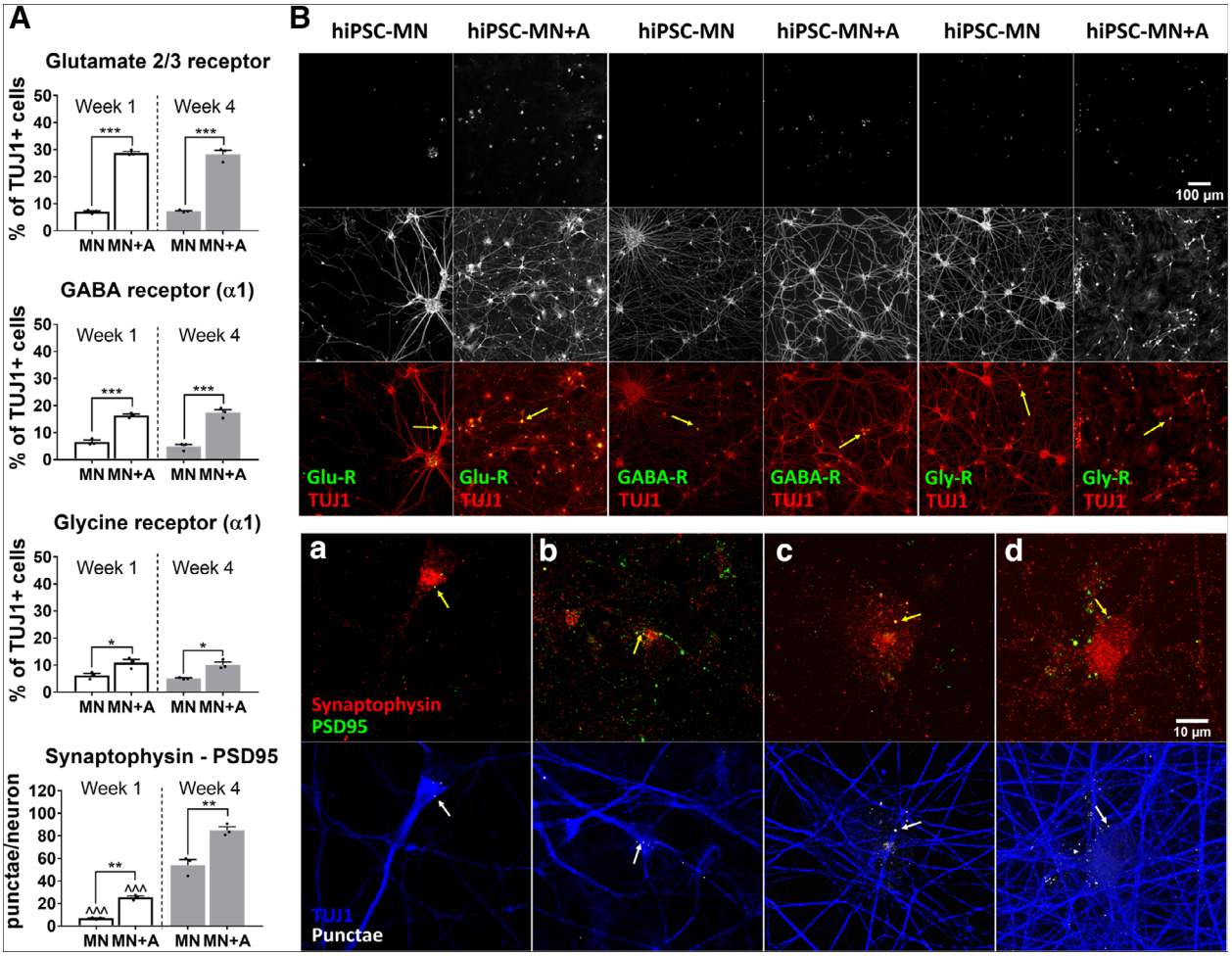

Figure 2. **(A):** Immunofluorescent quantification of neurotransmitter receptors and synapses. Neurotransmitter receptors (glutamate, gamma amino butyric acid [GABA], and glycine) were quantified as percentage of TUJ1 immunopositive cells (mean of n = 3 coverslips per culture condition and time point). Synapses were counted as colocalized punctae of synaptophysin, a presynaptic marker, and PSD95, a postsynaptic marker, per individual neuron (mean of n = 3 coverslips per condition, with a minimum of 10 neurons per coverslip). Human-induced pluripotent stem cell-derived motor neurons (hiPSC-MN) monocultures (MN) versus hiPSC-MN + hiPSC-derived astrocytes (hiPSC-A) cocultures (MN + A) were compared within each time point after plating (*), that is, week 1 (white bar) and week 4 (gray bar). Similarly, time point observations (week 1 vs. week 4) were compared within each condition (^).* or ^, $p < .05$; ** or ^^, $p < .01$; *** or ^^^, $p < .001$. **(B):** Representative immunohistochemical images for neurotransmitter receptors and synapses. Top: Immunoreactivity for receptors, that is, glutamate 2/3 receptor, GABA A receptor, and glycine receptor in hiPSC-MN + A cocultures compared with hiPSC-MN monocultures. Representative images were taken 1 week after plating. Bottom: Colocalized synaptophysin/PSD95 punctae per neuron in hiPSC-MN + A cocultures (b, d) compared with monocultures (a, c), from week 1 (a, b) to week 4 (c, d). Abbreviations: GABA-R, GABA A receptor; Glu-R, glutamate 2/3 receptor; Gly-R, glycine receptor.

We confirmed that spinal cord motor neuron identity, as defined by ChAT expression, is not significantly influenced by hiPSC-A coculture at either 60 or 90DIV nor is it influenced by coculture with mouse astrocytes. In contrast, the expression of genes required for the biosynthesis of neurotransmitter receptors (GRIA2, 3 for AMPA receptor, GABRA1 for GABA receptor, and GLRA1 for glycine receptor) and of GABA (GAD1) is particularly enriched in the cocultures with hiPSC-A, in a time-dependent manner (Supporting Information Fig. S5). We found that even though the presence of immature hiPSC-A or mouse astrocytes increased neuronal maturation when compared with hiPSC-MN monocultures, particularly at the later time point, this effect was consistently lower than that observed for cocultures with mature (i.e., cultured for 90DIV prior to use) human-derived astrocytes (Supporting Information Fig. S5).

hiPSC-MN Influence hiPSC-A Maturation

We sought to investigate astrocyte–neuron interactions in our human spinal cord iPSC-based platform, as their reciprocal maturation could dynamically influence the electrophysiological activity of hiPSC-MN recorded by MEA.

Confirming previous descriptions by Roybon et al. [15] and by our group [24], we defined a maturing glial identity of our hiPSC-A, as shown by immunoreactivity of cells for S100β (78.9% ± 4.2%), GFAP (41.2% ± 3.3%), EAAT2 (8.1% ± 1.6%), and Cx43 (22.7% ± 2.5%; Fig. 3). Spinal cord regional identity was suggested by high immunoreactivity (92.5% ± 1.4%) for HOXB4 (Supporting Information Fig. S3B). These astrocytes did not show relevant immunoreactivity for CD51 (4.1% ± 0.2%), a marker recently associated with a cortical identity [25] (Supporting Information Fig. S3B).

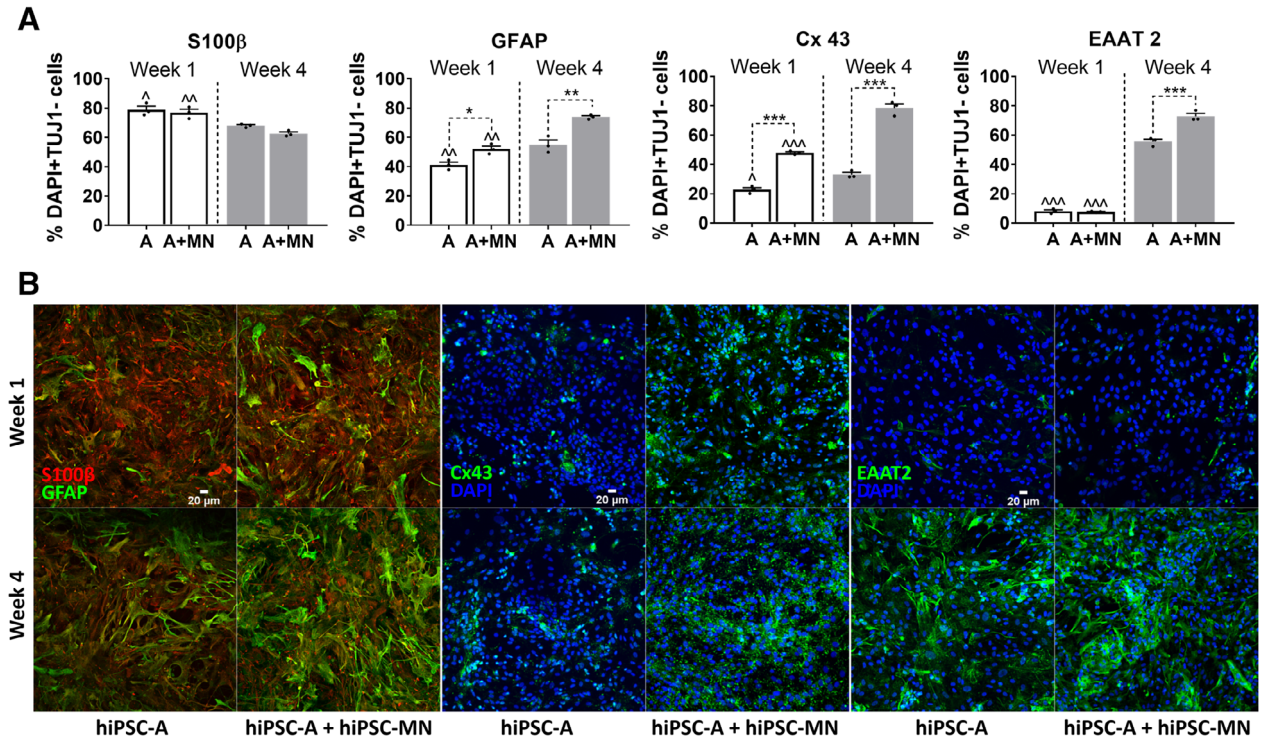

Figure 3. **(A):** Immunofluorescence quantification of astrocyte-specific markers. We considered the total number of DAPI$^+$ cells which were negative for TUJ1 immunostaining as an approximation of the number of astrocytes in human-induced pluripotent stem cell-derived astrocytes (hiPSC-A) + motor neurons (MN) cocultures (A + MN), and hiPSC-A monocultures (A); astrocyte-specific markers are expressed as percentage of DAPI$^+$ and TUJ1$^-$ cells. S100β$^+$ marks a less mature stage of astrocytic differentiation. Conversely, GFAP, Cx43, and EAAT2 are markers of maturing/mature astrocytes. Experimental conditions (hiPSC-A monocultures vs. hiPSC-MN + hiPSC-A cocultures) are compared within each time point (*). Time point observations (week 1 vs. week 4) are compared within each condition (^). * or ^, $p < .05$; ** or ^^, $p < .01$; *** or ^^^, $p < .001$). **(B):** Representative immunohistochemical images of astrocyte markers. Reciprocal changes of S100β and GFAP according to culture conditions and time in vitro. Immunoreactivity for Cx43 and EAAT2 in hiPSC-A monoculture and coculture, at week 1 and week 4 after plating.

We then found that the coculture of hiPSC-A with hiPSC-MN, when compared with hiPSC-A monocultures, increased the immunoreactivity for GFAP (52.0% ± 3.5%, $p < .01$), and Cx43 (47.9% ± 1.2%, $p < .001$), thus suggesting a more mature astrocyte phenotype. This enhanced glial maturation was even more marked after 4 weeks of coculture, when, in addition to GFAP (73.9% ± 1.6% vs. 54.9% ± 5.6%, $p = .001$) and Cx43 (78.5% ± 4.8% vs. 47.9% ± 1.2%, $p < .001$), EAAT2 immunoreactivity increased significantly (72.9% ± 3.5% vs. 55.6% ± 2.9%, $p < .001$; Fig. 3).

The qPCR experiments confirmed the trends observed with immunostaining at mRNA expression levels and on a larger set of astrocyte genes, which included also AQP4 and ALDH1L1. Some disparities between qPCR and ICC findings were evident, notably: Cx43 expression was comparable between monocultures and cocultures at week 1 and EAAT2 mRNA levels were not detected at week 1.

We used the qPCR platform to examine less mature hiPSC-A cultured for only 60DIV prior to use, and to investigate their maturation in the presence of hiPSC-MN. One week after their plating in coculture, qPCR experiments suggested an immature status of this glial population when compared with "mature" (i.e., 90DIV) hiPSC-A in monoculture and coculture. After 4 weeks of coculture, these cells remained significantly less mature, particularly when considering EAAT2 and GFAP expression levels, which were negligible. AQP4 and particularly Cx43 were two exceptions, as their expression levels in immature hiPSC-A were comparable for AQP4, or even higher for Cx43 ($p < .001$), than the more mature hiPSC-A (cultured for 90DIV prior to use) in monoculture or coculture (Supporting Information Fig. S6).

MEA Models hiPSC-A and hiPSC-MN Interactions

Given the striking hiPSC-A-dependent changes in hiPSC-MN maturation by immunofluorescence and qPCR, we sought to determine whether these structural changes and altered expression profiles are meaningfully related to altered electrophysiologic function of neurons. We plated hiPSC-MN in monocultures or cocultures with astrocytes on MEA plates that were either plated concurrently or serially. We recorded from the MEA plates at 1, 2, 3, and 4 weeks after plating (Fig. 4). We noted increases in all electrophysiological parameters evaluated (spike frequency, burst rate, percentage of electrodes spiking, and percentage of electrodes bursting) over time (Fig. 4A–4D). The changes over time occurred for all culture conditions (hiPSC-A/hiPSC-MN simultaneous coculture, hiPSC-MN followed by hiPSC-A, hiPSC-A followed by hiPSC-MN, and hiPSC-MN culture alone; $p < .001$ for week 1 vs. week 4 comparisons). However, the difference in the maturation between simultaneously cultured hiPSC-A and hiPSC-MN when

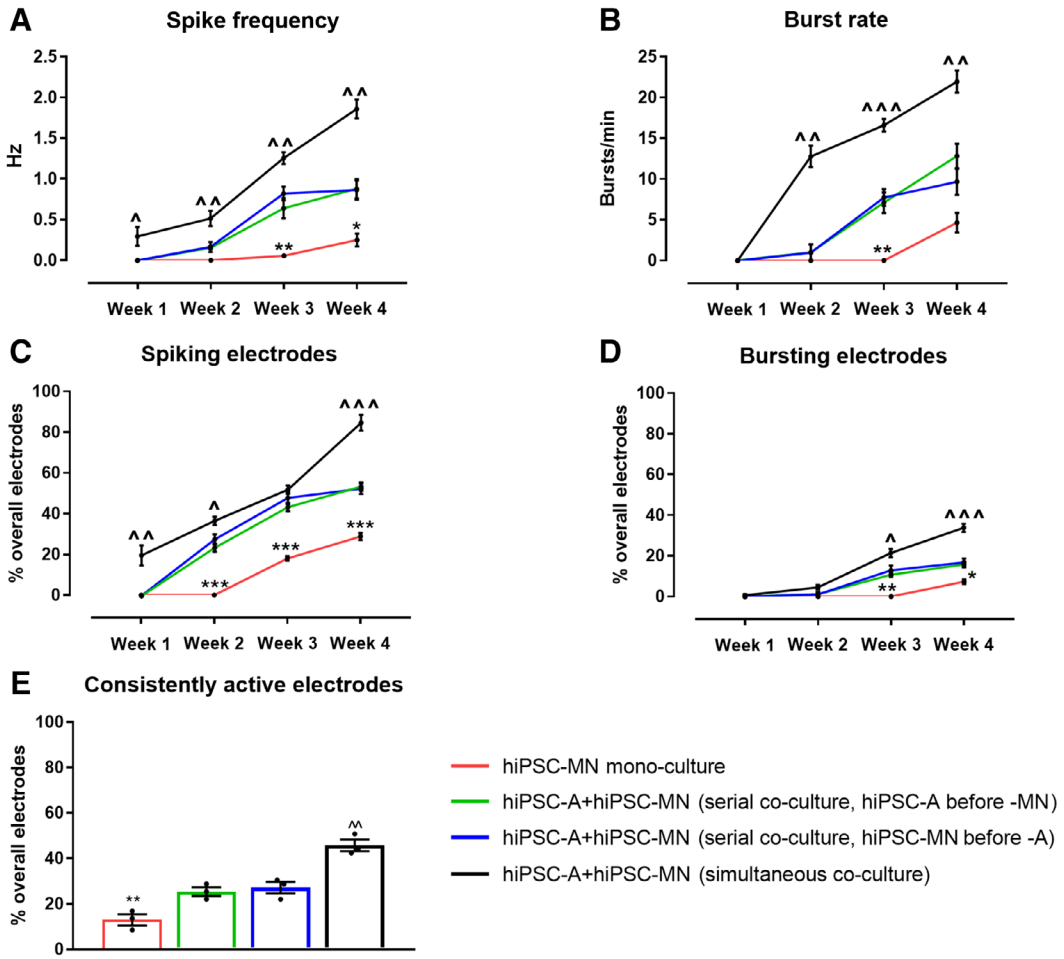

Figure 4. The electrophysiological maturation of human-induced pluripotent stem cell-derived motor neurons (hiPSC-MN) by hiPSC-derived astrocytes (hiPSC-A) over time. **(A–D):** Electrophysiological parameters were recorded at weekly intervals for hiPSC-MN in monoculture as well in coculture with hiPSC-A. Data are presented as mean ± SEM (mean of $n = 3$ multielectrode array [MEA] plates). **(E):** The percentage of consistently active electrodes represents populations of neurons with stable electrophysiological activity over individual electrodes ($n = 3$ cultures). Comparisons of hiPSC-MN monocultures with the two hiPSC-MN/A serial cocultures (*). Comparisons between the simultaneous coculture and the two serial cocultures (^). * or ^, $p < .05$; ** or ^^, $p < .01$; *** or ^^^, $p < .001$.

compared with hiPSC-MN cultured alone was most dramatic with the spike frequency, burst rate, number of spiking, and number of bursting electrodes higher in the simultaneous coculture at all time points. Although less marked and uniform over time points, the simultaneous cocultures also showed greater degrees of neuronal activity when compared with serial cocultures. We did not see any evidence of spontaneous synchronous bursting activity, which is thought to reflect high degrees of neuronal connectivity [18, 26] (not shown). For all conditions, MEA plates with hiPSC-A alone were recorded as controls, and did not show any measurable electrophysiological activity within the 4-week period of recording, confirming the relatively pure composition of our astrocyte cultures (Supporting Information Fig. S3B). We calculated the percentage of active electrodes whose spike activity persisted throughout the 4 weeks of recordings and defined this parameter as "consistently active electrodes" (Fig. 4E). We noted that electrophysiological consistency was influenced by the sequence of culturing hiPSC-A and hiPSC-MN. Indeed, approximately 45.8% ± 4.4% of electrodes remained persistently active over 4 weeks following the simultaneous culture of iPSC-A and iPSC-MN. The culture of either hiPSC-A first (25.4% ± 3.4%) or hiPSC-MN first (27.1% ± 4.5%) were not significantly different from each other, but had lower electrophysiological consistency than the simultaneous culture ($p < .05$). Furthermore, only 13.0% ± 4.2% of electrodes showed persistent spike activity when hiPSC-MN were cultured in the absence of hiPSC-A ($p < .001$; Fig. 4E).

In addition to the 4 week recordings, we tested the long-term survival of our optimized coculture, and succeeded in maintaining these cells in culture for up to 9 months. A trending increase in spike frequency was noted over time (Supporting Information Fig. S7). This is consistent with data derived from cortical hiPSC-neurons (hiPSC-N) [6].

We also examined whether the plating density of hiPSC-A influences hiPSC-MN activity (Fig. 5A). The spike frequency, percentages of electrodes exhibiting spikes, and percentages of electrodes exhibiting bursts were significantly increased across all time points in cocultures with a density of 1×10^5 astrocytes per plate when compared with a lower density of 0.5×10^5

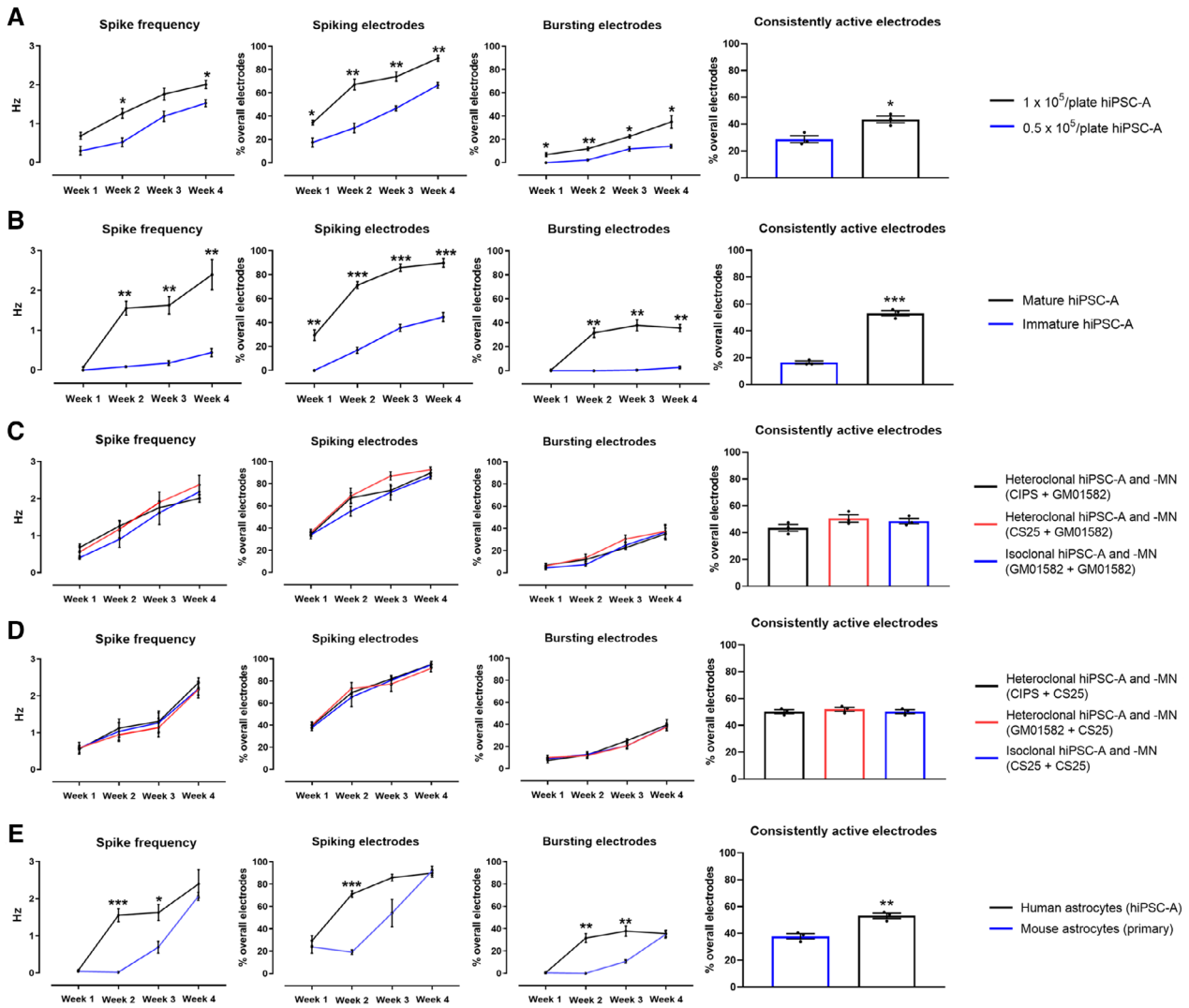

Figure 5. Astrocyte variables influencing the electrophysiological maturation of human-induced pluripotent stem cell-derived motor neurons (hiPSC-MN) in coculture. **(A):** Influence of hiPSC-derived astrocytes (hiPSC-A) density on the electrophysiological maturation of hiPSC-MN as measured by multielectrode array (MEA). **(B):** Effect of immature versus mature astrocytes on neuronal maturation as measured by MEA. **(C, D):** Influence of hiPSC-A and hiPSC-MN respective iPSC-line origin on the electrophysiological maturation of hiPSC-MN. The source of hiPSC-MN was the control GM01582 line in (C), and the control CS25 line in (D). In both figures, MN were cocultured with control hiPSC-A lines (CIPS, CS25, and GM01582 lines). **(E):** Effect of the species origin (mouse primary spinal cord astrocytes vs. human iPSC-A) on hiPSC-MN maturation, as recorded by MEA. Data are the mean of $n = 3$ MEA plates for all conditions. *, $p < .05$; **, $p < .01$; ***, $p < .001$.

astrocytes per plate. However, when even higher densities of astrocytes (2×10^5 astrocytes per plate) were used, there was poor cell adhesion immediately after plating, which led to lifting of the cultures (not shown). These findings were correlated with a higher percentage of "consistently active electrodes" in the cocultures with 1×10^5 astrocytes per plate when compared with a lower density of 0.5×10^5 astrocytes per plate (43.6% $\pm$ 2.4% vs. 28.8% $\pm$ 2.6%, $p < .05$).

To assess whether astrocyte age and maturity prior to coculture with hiPSC-MN would influence hiPSC-MN electrophysiological activity, we cultured hiPSC-A for 60 days prior to the coculture with hiPSC-MN. When compared to cocultures with mature (90DIV) hiPSC-A, these cells had a significantly reduced capacity to support hiPSC-MN spike frequency and number of active electrodes (Fig. 5B). This phenomenon persisted over the 4-week time course ($p < .05$ for all comparisons). We also observed that the presence of immature hiPSC-A determined reduced consistency of neuronal firing (53.1% $\pm$ 2.0% vs. 16.4% $\pm$ 1.1%, $p < .001$).

Given that, using hiPSC raises the question as to whether there could be variations in electrophysiological properties amongst different iPSC lines, we compared simultaneous cocultures that were "isoclonal" (hiPSC-A and -MN differentiated from the same GM01582 line) or "heteroclonal" (hiPSC-A from CIPS line or CS 25 line and hiPSC-MN from GM01582 line). We did not appreciate significant line-specific differences in electrophysiological activity over time (Fig. 5C); this was paralleled by similar percentages of consistently active electrodes (43.5% $\pm$ 4.3%, 50.6% $\pm$ 4.7%, and 48.6% $\pm$ 3.5%). We confirmed these observations using another hiPSC-MN line (i.e., CS25), and recording from isoclonal versus heteroclonal cocultures (Fig. 5D).

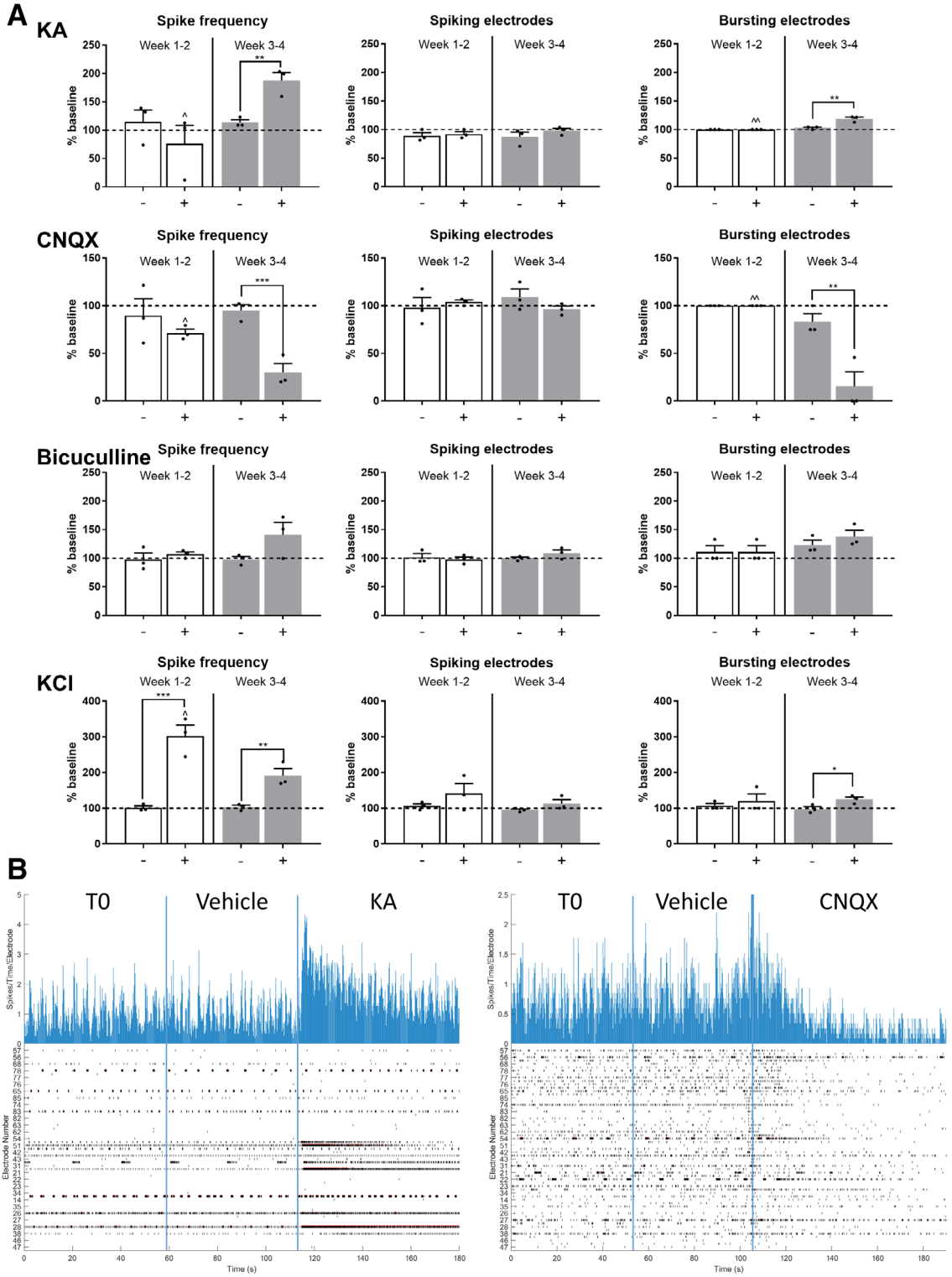

Figure 6. Human-induced pluripotent stem cell-derived astrocytes (hiPSC-A) influence the responses of hiPSC-derived motor neurons (hiPSC-MN) to neurotransmitters. **(A):** hiPSC-MN responses to compounds acting on neurotransmitter receptors (KA, cyanquixaline [CNQX], and bicuculline) and to a nonspecific depolarizing agent (KCl), in hiPSC-MN/-A cocultures, over time (week 1–2 after plating—white bars and week 3–4 after plating—gray bars). The activity recorded by MEA plates after vehicle addition (–) and after drug addition (+) was normalized to the baseline activity (horizontal dashed line; mean of $n = 3$ independent experiments per drug and time point). Comparisons between activity after vehicle and after drug addition (*). Time point observations (week 1–2 vs. week 3–4) are compared within each condition (^). * or ^, $p < .05$; ** or ^^, $p < .01$; *** or ^^^, $p < .001$. **(B):** Sample of real-time recording of hiPSC-MN/hiPSC-A cocultures by MEA. Two representative recordings of electrophysiological activity are shown: the effect of the addition of KA (left) and CNQX (right) compared with the addition of the vehicle and to baseline activity. Top histograms represent the number of spikes per electrode and per time point of recording, whereas the bottom raster plots represent overall electrodes showing spiking activity per time point. Abbreviations: KA, kainic acid; KCl, potassium chloride.

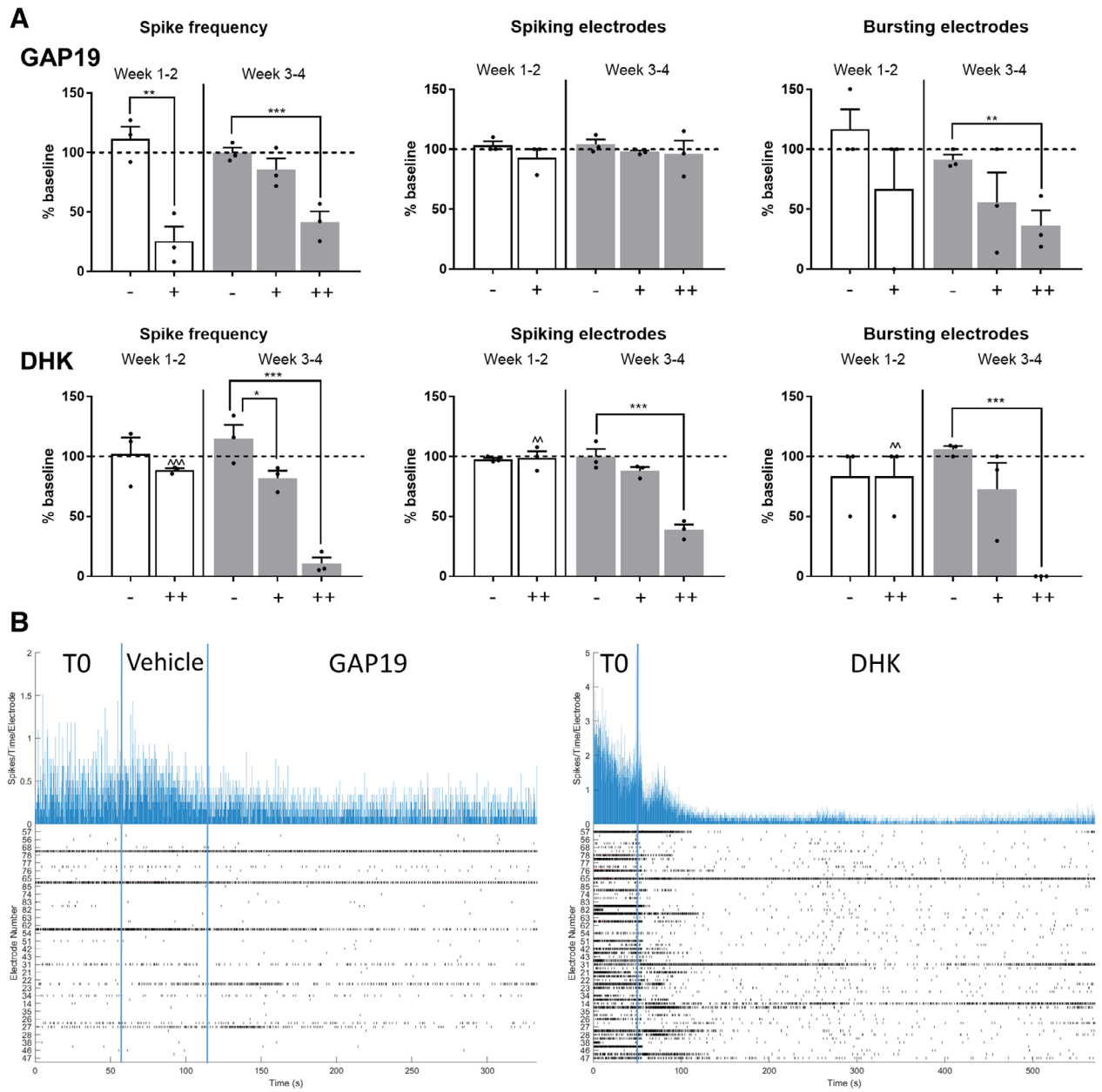

Figure 7. Compounds targeting astrocytes affect human-induced pluripotent stem cell-derived motor neurons (hiPSC-MN) electrophysiology as recorded by multielectrode array (MEA). **(A):** Effects of GAP19, a specific Cx43 hemichannel blocker, on neuronal activity, in hiPSC-MN/-A cocultures, over time (week 1–2 after plating—white bars, and week 3–4 after plating—gray bars; –, vehicle; +, 34 μM; ++, 340 μM). Changes on hiPSC-MN electrophysiological activity after the addition of DHK (–, vehicle; +, 50 μM; ++, 300 μM). The electrophysiological parameters were normalized to the baseline activity recorded for 1 minute (dashed line; mean of $n = 3$ independent experiments per drug and per time point; * or ^, $p < .05$; ** or ^^, $p < .01$; *** or ^^^, $p < .001$). **(B):** Representative MEA raster plots of electrophysiological activity following the addition of GAP19 (left) and DHK (right). Abbreviation: DHK, dihydrokainic acid.

Most studies utilizing MEA for recording from human iPSC-neurons have used rodent astrocytes in the context of coculture systems [6, 8]. Our results demonstrate that mouse spinal cord astrocytes resulted in a slower maturation of the electrophysiological activity of hiPSC-MN when compared with cocultures with hiPSC-A. MEA activity became comparable between these two conditions only after 4 weeks of coculture. Overall, the percentage of consistently active electrodes was reduced in the mouse/human cocultures (37.8% ± 2.0% vs. 53.1% ± 2.0%, $p < .01$; Fig. 5E).

MEA as a Screening Platform for Drugs Targeting hiPSC-MN and hiPSC-A

Beyond the spontaneous electrophysiological activities of hiPSC-MN, we examined the response of these cells, in monoculture or coculture, to compounds targeting ion channels and neurotransmitter receptors. When cultured alone, hiPSC-MN responded to the application of 100 mM of potassium chloride (KCl), a nonspecific depolarizing agent, with an increase in spike frequency without any change in the number of spiking or bursting electrodes (Supporting Information Fig. S8).

However, the application of neurotransmitter agonists/antagonists did not alter MEA electrophysiological parameters (Supporting Information Fig. S8).

In contrast, when recording from hiPSC-A/hiPSC-MN simultaneous cocultures (Fig. 6), we found that the AMPA/kainate receptor agonist, KA, and antagonist, CNQX, induced appropriate (i.e., an increase for KA and a decrease for CNQX) changes in the spike frequency together with a significant variation of bursting activity. These responses were time-dependent, as they were absent at earlier stages of maturation in vitro (week 1–2 after plating), while they appeared after 3–4 weeks of coculture. The addition of bicuculline, a GABA antagonist, did not significantly change the overall MEA activity, although there was a trend toward increased spike frequency and percentage of bursting electrodes in older cocultures. In contrast to the neurotransmitter modulators, KCl showed depolarizing effects across all time points (Fig. 6). We did not observe any hypersynchronous bursting activity occurring after the application of any of these compounds.

We used this screening platform to test the effect of neurotransmitter agonists/antagonists on cocultures of hiPSC-MN with mouse primary spinal cord astrocytes (Supporting Information Fig. S9). In contrast to fully human cocultures, we did not observe significant electrophysiological responses to drugs acting on neurotransmitter receptors, although a trend of increased activity in response to KA and bicuculline and reduced activity after the application of CNQX was evident.

To examine the immediate effect of altered astrocyte function on neuronal firing, we used our MEA platform to test compounds targeting astrocyte specific transporters, and evaluate their indirect influence on neuronal firing. The application of GAP19, a connexin 43 hemichannel blocker, resulted in a significant reduction of MEA activity (spike frequency and bursting electrodes). This phenomenon was apparent across all time points of coculture and was dose-dependent (Fig. 7). To ensure that this effect was mediated by astrocytes, we tested the drug on hiPSC-MN monocultures, and did not appreciate any variation in neuronal activity (Supporting Information Fig. S8). The selective glutamate transporter (EAAT2) antagonist, DHK, caused a reduction in MEA activity, which appeared within 10 minutes of recording. This effect was dose-dependent, and could be appreciated only in coculture at later time points (weeks 3–4; Fig. 7).

Discussion

To the best of our knowledge, this study is the first to investigate how hiPSC-derived glia, differentiated into a distinct spinal cord astrocyte identity [15], influence the morphological, molecular, electrophysiological and pharmacological properties of hiPSC-MN in a MEA-based platform. The regional specificity of this paradigm is particularly relevant in precision medicine strategies for modeling neurological diseases. Previous literature on MEA applied to hiPSC studies have relied exclusively upon hiPSC-derived cortical neurons, for in vitro modeling of epilepsy and seizures [7, 8]. Although recent MEA studies have used neurons cocultured with human iPSC-derived astrocytes [4, 7–9], less attention has been given to how astrocytes may influence neuronal electrophysiological activity—particularly in the context of human biology.

To establish a hiPSC platform of spinal cord astrocyte/MN coculture, we first optimized the sequence of coculture. As observed by others [27], the culture of hiPSC-MN in the absence of astrocytes resulted in a significant number of large aggregates of iPSC-MN that morphologically made it difficult to discern specific boundaries and connections amongst these cells. Furthermore, these cultures demonstrated diffuse neuronal mobility, as reflected electrophysiologically by a low number of electrodes with persistent activity for the 4-weeks recording period. The culture of either hiPSC-A followed by plating of hiPSC-MN or the converse, resulted in fewer neuronal aggregates and an increase in the number of MEA electrodes showing persistent activity. Finally, we observed that the simultaneous plating of hiPSC-A and hiPSC-MN morphologically resulted in a much more homogeneous distribution of hiPSC-MN, and in the greatest number of electrodes showing persistent activity.

The observation that neuronal subtypes and cell densities (both glial and neuronal) did not change over time, made us more confident that the neuronal activity, as recorded by MEA, was a reflection of neuronal maturation. A stable composition of hiPSC-derived neuronal subtypes over time has been observed by others [23], and may reflect an early determination of neuronal subtypes during neural progenitor cell differentiation. Our data suggest that the majority of our cells are spinal cord motor neurons (positive for ChAT and, to a lesser extent, for ISL1/2), expressing appropriate neurotransmitter receptors, with AMPA receptors being more represented than GABA and glycine receptors, as would be expected in the spinal cord. Importantly, in accordance with our protocol of ventralization and caudalization, and in contrast to previous studies involving hiPSC-cortical neurons [7, 8], only a very small percentage of neurons were corticospinal $CTIP2^{+}$ motor neurons. Neuronal maturation overtime, and particularly in the presence of astrocytes, was reflected morphologically by increased cell soma and neurite sizes, and by increased number and complexity of neurites. These features determine an enhanced ability of individual neurons to generate action potentials and to synapse with neighboring cells [28]. The degree of morphological maturation of our neuronal population resembles that of MN derived from human embryonic stem cells [29] and of cortical hiPSC-N [6, 8], although it is still reduced when compared with the human alpha motor neurons in adults [30, 31].

We used this optimized coculture platform for MEA recording to examine hiPSC-A contributions to motor neuron electrophysiology. We observed that astrocytes influenced hiPSC-MN electrophysiology over time with increases in spiking and bursting activity that far exceeded the activity of hiPSC-MN cultured in the absence of astrocytes. These findings are consistent with previous observations on human iPSC-derived cortical neurons [4, 9, 32–38]. Moreover, the spike frequencies we recorded are comparable to those reported by MEA studies with cortical hiPSC-N [6, 8, 39] or with rodent primary MN [36, 40, 41]. These firing rates are lower than those observed in vivo and probably reflect reduced neuromodulatory influences from afferent or descending inputs [42, 43]. In contrast to MEA studies utilizing cortical neurons [4, 8, 40, 41], we did not appreciate the presence of synchronized bursting activity among spinal cord hiPSC-MN up to 9 months of culture in vitro. Given that, morphologically we

appreciate evidence of complex networks and well-developed synapses, the lack of these patterns may suggest a regional difference between cortical and spinal cord hiPSC-MN and/or -A. Organotypic cultures and dissociated cells from rodent spinal cords disclose patterns of rhythmic bursting activity, which resemble the oscillatory patterns of locomotion in vivo or the "fictive locomotion" activity recorded from spinal cord preparations in vitro, and may be generated by the same locomotor networks and/or neuronal subtypes [44]. The neurochemical basis of similar patterns, with potential roles of GABA, glycine and NMDA receptors [41, 45], and their neuronal contributors, with recent identification of rhythm-generating excitatory interneurons (such as rodent CHX10+ and SHOX2+ interneurons) [46] represent a field of ongoing research, which may benefit from a MEA and fully human spinal cord platform, although they were not the focus of this study [47, 48].

We then determined that the ratio of hiPSC-A to hiPSC-MN influenced the activity of MN with higher concentrations of hiPSC-A providing a significant increase in hiPSC-MN firing. The significantly lower hiPSC-MN firing when cultured with 60-day astrocytes, which was paralleled by qPCR profiling of hiPSC-MN, suggest that for the purposes of examining electrophysiological activity, more mature astrocytes seem to be essential.

One of the concerns regarding the use of human iPSCs, as opposed to rodent astrocytes, is that genetic heterogeneity among individuals is much greater than in rodents thus making interpretation of results more challenging. Our data provide early evidence that the source of control iPSC-derived astrocytes does not significantly influence iPSC-MN activity. Similarly, we observed similar degrees of MEA activity independently of the source of hiPSC-MN. In order to confirm these observations, a larger set of hiPSC-A/-MN lines and their potential combinations will be needed in future studies.

Given that hiPSC-A differentiation requires longer time in culture, generates less mature astrocytes, and produces fewer astrocytes than primary rodent-derived astrocytes, we examined whether there was a difference in neuronal activity of cocultures with hiPSC-A compared with mouse primary spinal cord astrocytes. We found that rodent spinal cord astrocytes resulted in a delayed pattern of hiPSC-MN electrophysiological maturation when compared with hiPSC-A. This difference paralleled qPCR profiling showing that the maturation of hiPSC-MN was less robust when mouse astrocytes were used and pharmacological testing showing only modest responses to drugs acting on neurotransmitter receptors in human/mouse cocultures This appears to be related to species differences rather than regional heterogeneity since rodent astrocytes were derived from the spinal cord. Our findings are in contrast to those of Lischka et al. [49] who found that neonatal mouse cortical but not isogenic human astrocyte feeder layers enhanced the maturation of iPSC-N. It must be noted, however, that those investigators used a cortical patterning protocol to differentiate iPSC-N, mouse forebrains to derive rodent astrocytes, and a patch-clamp platform to record neuronal activity. Our observations may not be surprising as a growing body of evidence suggests that human astrocytes are more complex than their rodent counterparts, both morphologically [50] and physiologically [50, 51]. We did not directly compare molecular signatures of rodent astrocytes to hiPSC-A and, therefore, cannot exclude that other factors besides species-specific differences could explain our observations on neuronal maturation.

Essential to the validation of this coculture strategy was the demonstration that hiPSC-MN electrophysiological activity was not merely spontaneous but would also respond to the application of neurotransmitters and that their activity could be inhibited by receptor antagonists. Consistent with the identity of these cells as iPSC-MN, in our coculture platform we observed a robust and consistent response to AMPA receptor agonists/antagonists (KA and CNQX, respectively). As shown by others for hiPSC-cortical neurons [8, 9], this effect was maturation-dependent, as it appeared only after 3–4 weeks in vitro, whereas it was absent at earlier stages of maturation. The response to the GABA antagonist bicuculline was less robust, a finding consistent with a lower representation of GABA receptors. In contrast, neuronal cultures without astrocytes did not show any response to neurotransmitter modulators, which is consistent with our observations on the immaturity of hiPSC-MN monocultures, and parallels previous findings on hiPSC-cortical neurons [4, 8, 27].

Interestingly, the morphological and molecular characterization of our coculture platform showed that astrocyte maturation, as defined by different glial-specific markers, was enhanced by the presence of neurons. Even though the trends of glial markers were similar for both ICC and qPCR studies, some differences were noted, that can potentially be explained by a differential regulation of transcription, translation, or protein trafficking. We also found that astrocyte maturation was time dependent and marker dependent, as shown by the profile of maturation of "immature" hiPSC-A (i.e., hiPSC-A cultured for 60DIV prior to use) in coculture, which was less marked than 90DIV hiPSC-A, with, however, the exception of two markers, Cx43 and AQP4. These early changes in AQP4 and Cx43 profiles suggest a neuronal influence on their expression not related to astrocyte maturation, and parallels previous literature on rodent astrocytes showing elevations in calcium intercellular signaling [52, 53] and changes in astrocyte volume [54, 55] in response to neuronal activity.

In a previous study [24], we analyzed the transcriptomic profile of hiPSC-A after in vivo transplantation in the rat spinal cord, and found marked increases of GFAP, EAAT2, Cx43, and AQP4 [24]. Besides confirming these previous findings in vitro and in a fully human hiPSC-based platform, our data suggest that iPSC-A maturation in the spinal cord microenvironment may be, at least partially, determined by the presence of neurons.

Astrocyte–neuron crosstalk is relevant to our MEA platform since hiPSC-MN electrophysiological maturation may be influenced by the concurrent astrocyte maturation in coculture. This is supported by the observation that immature hiPSC-A in coculture with hiPSC-MN determined lower degrees of neuronal activity on MEA. Furthermore, the pharmacological effects of GAP19 and DHK on MEA activity paralleled hiPSC-A maturation in coculture: GAP19 was active in both early and late cocultures, which were characterized by a relatively high expression of Cx43, but higher concentrations of the drug were needed in older cultures in parallel to increased levels of Cx43. DHK showed significant effects only after 3–4 weeks of coculture, when EAAT2 expression became relevant. Although further experiments may be needed to clarify

the mechanism of Cx43 and DHK influences on neuronal firing, that were beyond the scope of this study, our data show the feasibility of a MEA-based platform for testing drugs specifically targeting astrocytes.

Conclusion

In this study, we demonstrate that hiPSC-A influence the morphological, molecular and electrophysiological maturation of hiPSC-MN. Similarly, we show that hiPSC-A maturation is enhanced by the presence of hiPSC-MN in coculture, thus allowing for a crosstalk that can be investigated with MEA. This fully human, spinal cord-specific, coculture platform with MEA analyses, provides a new tool for investigating astrocyte/MN interactions and for screening pharmacological compounds and has the potential to more accurately model human diseases with spinal cord pathology, including spinal muscular atrophy and amyotrophic lateral sclerosis.

Acknowledgments

We thank Labchan Rajbhandari and Dr. Venkatesan's Lab who provided the plasma cleaning platform. Funding was provided by the Packard Center for ALS Research at Johns Hopkins (N.J.M.), Department of Defense, W81XWH1810175 (N.J.M.), ALS Association 18-DDC-436 (N.J.M.), and NIH K12NS09848 (C.H.).

Author Contributions

A.T.: conception and design, collection and/or assembly of data, data analysis and interpretation, manuscript writing; R.D., C.H.: conception and design, collection and/or assembly of data, data analysis and interpretation; J.J., J.-P.R., S.K.G.: collection and/or assembly of data, data analysis and interpretation; G.L.: data analysis and interpretation; G.L.: provision of study material; N.H.: conception and design; N.J.M.: conception and design, collection and/or assembly of data, data analysis and interpretation, manuscript writing, financial support, final approval of manuscript.

Disclosure of Potential Conflicts of Interest

The authors indicated no potential conflicts of interest.

Data Availability Statement

The data that support the findings of this study are available from the corresponding author upon reasonable request.

References

1 Richard JP, Maragakis NJ. Induced pluripotent stem cells from ALS patients for disease modeling. Brain Res 2015;1607:15–25.

2 Grainger AI, King MC, Nagal DA, et al. In vitro models for seizure-liability testing using induced pluripotent stem cells. Front Neurosci 2018;12:590.

3 Bardy C, van den Hurk M, Eames T, et al. Neuronal medium that supports basic synaptic functions and activity of human neurons in vitro. Proc Natl Acad Sci USA 2015; 112:E2725–E2734.

4 Kayama T, Suzuki I, Odawara A, et al. Temporally coordinated spiking activity of human induced pluripotent stem cell-derived neurons co-cultured with astrocytes. Biochem Biophys Res Commun 2018;495:1028–1033.

5 Hofrichter M, Nimtz L, Tigges J, et al. Comparative performance analysis of human iPSC-derived and primary neural progenitor cells (NPC) grown as neurospheres in vitro. Stem Cell Res 2017;25:72–82.

6 Odawara A, Katoh H, Matsuda N, et al. Physiological maturation and drug responses of human induced pluripotent stem cell-derived cortical neuronal networks in long-term culture. Sci Rep 2016;6:26181.

7 Ishii MN, Yamamoto K, Shoji M, et al. Human induced pluripotent stem cell (hiPSC)-derived neurons respond to convulsant drugs when co-cultured with hiPSC-derived astrocytes. Toxicology 2017;389:130–138.

8 Odawara A, Matsuda N, Ishibashi Y, et al. Toxicological evaluation of convulsant and anticonvulsant drugs in human induced pluripotent stem cell-derived cortical neuronal networks using an MEA system. Sci Rep 2018;8:10416.

9 Tukker AM, Wijnolts FMJ, de Groot A, et al. Human iPSC-derived neuronal models for in vitro neurotoxicity assessment. Neurotoxicology 2018;67:215–225.

10 Clarke LE, Barres BA. Emerging roles of astrocytes in neural circuit development. Nat Rev Neurosci 2013;14:311–321.

11 Tyzack G, Lakatos A, Patan R, et al. Human stem cell-derived astrocytes: Specification and relevance for neurological disorders. Curr Stem Cell Rep 2016;2:236–247.

12 Denis-Donini S, Glowinski J, Prochiantz A, Glial heterogeneity may define the three-dimensional shape of mouse mesencephalic dopaminergic neurones. Nature 1984;307: 641–643.

13 Donnelly CJ, Zhang PW, Pham JT, et al. RNA toxicity from the ALS/FTD C9ORF72 expansion is mitigated by antisense intervention. Neuron 2013;80:415–428.

14 Boulting GL, Kiskinis E, Croft GF, et al. A functionally characterized test set of human induced pluripotent stem cells. Nat Biotechnol 2011;29:279–286.

15 Roybon L, Lamas NJ, Garcia AD, et al. Human stem cell-derived spinal cord astrocytes with defined mature or reactive phenotypes. Cell Rep 2013;4:1035–1048.

16 Miller SJ, Philips T, Kim N, et al. Molecularly defined cortical astroglia subpopulation modulates neurons via secretion of Norrin. Nat Neurosci 2019;22:741–752.

17 Almad AA, Doreswamy A, Gross SK, et al. Connexin 43 in astrocytes contributes to motor neuron toxicity in amyotrophic lateral sclerosis. Glia 2016;64:1154–1169.

18 Huang YT, Chang YL, Chen CC, et al. Positive feedback and synchronized bursts in neuronal cultures. PLoS One 2017;12: 0187276.

19 Krzisch M, Temprana SG, Mongiat LA, et al. Pre-existing astrocytes form functional perisynaptic processes on neurons generated in the adult hippocampus. Brain Struct Funct 2015;220:2027–2042.

20 Liang X, Song MR, Xu Z, et al. Isl1 is required for multiple aspects of motor neuron development. Mol Cell Neurosci 2011;47: 215–222.

21 Cao SY, Hu Y, Chen C, et al. Enhanced derivation of human pluripotent stem cell-derived cortical glutamatergic neurons by a small molecule. Sci Rep 2017;7:3282.

22 Mower GD, Guo Y. Comparison of the expression of two forms of glutamic acid decarboxylase (GAD67 and GAD65) in the visual cortex of normal and dark-reared cats. Brain Res Dev Brain Res 2001;126:65–74.

23 Kang S, Chen X, Gong S, et al. Characteristic analyses of a neural differentiation model from iPSC-derived neuron according to morphology, physiology and global gene expression pattern. Sci Rep 2017;7:12233.

24 Haidet-Phillips AM, Roybon L, Gross SK, et al. Gene profiling of human induced pluripotent stem cell-derived astrocyte progenitors following spinal cord engraftment. Stem Cells Translational Medicine 2014;3: 575–585.

25 John Lin CC, Yu K, Hatcher A, et al. Identification of diverse astrocyte populations and their malignant analogs. Nat Neurosci 2017;20:396–405.

26 Penn Y, Segal M, Moses E. Network synchronization in hippocampal neurons. Proc Natl Acad Sci USA 2016;113:3341–3346.

27 Kuijlaars J, Oyelami T, Diels A, et al. Sustained synchronized neuronal network activity in a human astrocyte co-culture system. Sci Rep 2016;6:36529.

28 Grudt TJ, Perl ER. Correlations between neuronal morphology and electrophysiological features in the rodent superficial dorsal horn. J Physiol 2002;540:189–207.

29 Takazawa T, Croft GF, Amoroso MW, et al. Maturation of spinal motor neurons derived from human embryonic stem cells. PLoS One 2012;7:40154.

30 Tomlinson BE, Irving D, Rebeiz JJ. Total numbers of limb motor neurones in the human lumbosacral cord and an analysis of the accuracy of various sampling procedures. J Neurol Sci 1973;20:313–327.

31 Stephens B, Guiloff RJ, Navarrete R, et al. Widespread loss of neuronal populations in the spinal ventral horn in sporadic motor neuron disease. A morphometric study. J Neurol Sci 2006;244:41–58.

32 Odawara A, Saitoh Y, Alhebshi AH, et al. Long-term electrophysiological activity and pharmacological response of a human induced pluripotent stem cell-derived neuron and astrocyte co-culture. Biochem Biophys Res Commun 2014;443: 1176–1181.

33 Fukushima K, Miura Y, Sawada K, et al. Establishment of a human neuronal network assessment system by using a human neuron/astrocyte co-culture derived from fetal neural stem/progenitor cells. J Biomol Screen 2016;21:54–64.

34 Tang X, Zhou L, Wagner AM, et al. Astroglial cells regulate the developmental timeline of human neurons differentiated from induced pluripotent stem cells. Stem Cell Res 2013;11:743–757.

35 Qi Y, Zhang XJ, Renier N, et al. Combined small-molecule inhibition accelerates the derivation of functional cortical neurons from human pluripotent stem cells. Nat Biotechnol 2017;35:154–163.

36 Black BJ, Atmaramani R, Pancrazio JJ. Spontaneous and evoked activity from murine ventral horn cultures on microelectrode arrays. Front Cell Neurosci 2017;11:304.

37 Sabitha KR, Sanjay D, Savita B, et al. Electrophysiological characterization of Nsc-34 cell line using microelectrode array. J Neurol Sci 2016;370:134–139.

38 Geissler M, Faissner A. A new indirect co-culture set up of mouse hippocampal neurons and cortical astrocytes on microelectrode arrays. J Neurosci Methods 2012;204: 262–272.

39 Gunhanlar N, Shpak G, van der Kroeg M, et al. A simplified protocol for differentiation of electrophysiologically mature neuronal networks from human induced pluripotent stem cells. Mol Psychiatry 2018;23:1336–1344.

40 Streit J, Tscherter A, Heuschkel MO, et al. The generation of rhythmic activity in dissociated cultures of rat spinal cord. Eur J Neurosci 2001;14:191–202.

41 Tscherter A, Heuschkel MO, Renaud P, et al. Spatiotemporal characterization of rhythmic activity in rat spinal cord slice cultures. Eur J Neurosci 2001;14:179–190.

42 Button, DC, Gardiner K, Marqueste T, et al. Frequency-current relationships of rat hindlimb alpha-motoneurones. J Physiol 2006;573:663–677.

43 Carp JS, Tennissen AM, Mongeluzi DL, et al. An in vitro protocol for recording from spinal motoneurons of adult rats. J Neurophysiol 2008;100:474–481.

44 Beato M, Nistri A. Interaction between disinhibited bursting and fictive locomotor patterns in the rat isolated spinal cord. J Neurophysiol 1999;82:2029–2038.

45 Legrand JC, Darbon P, Streit J. Contributions of NMDA receptors to network recruitment and rhythm generation in spinal cord cultures. Eur J Neurosci 2004;19: 521–532.

46 Kiehn O. Decoding the organization of spinal circuits that control locomotion. Nat Rev Neurosci 2016;17:224–238.

47 Kiehn O, Dougherty KJ, Hägglund M, et al. Probing spinal circuits controlling walking in mammals. Biochem Biophys Res Commun 2010;396:11–18.

48 Husch A, Cramer N, Harris-Warrick RM. Long-duration perforated patch recordings from spinal interneurons of adult mice. J Neurophysiol 2011;106:2783–2789.

49 Lischka FW, Efthymiou A, Zhou Q, et al. Neonatal mouse cortical but not isogenic human astrocyte feeder layers enhance the functional maturation of induced pluripotent stem cell-derived neurons in culture. Glia 2018;66:725–748.

50 Zhang Y, Sloan SA, Clarke LE, et al. Purification and characterization of progenitor and mature human astrocytes reveals transcriptional and functional differences with mouse. Neuron 2016;89:37–53.

51 Sun W, McConnell E, Pare JF, et al. Glutamate-dependent neuroglial calcium signaling differs between young and adult brain. Science 2013;339:197–200.

52 Verkhratsky A, Kettenmann H. Calcium signalling in glial cells. Trends Neurosci 1996; 19:346–352.

53 Newman EA. Glial cell inhibition of neurons by release of ATP. J Neurosci 2003; 23:1659–1666.

54 Bar El Y, Kanner S, Barzilai A, et al. Activity changes in neuron-astrocyte networks in culture under the effect of norepinephrine. PLoS One 2018;13:0203761.

55 Xie L, Kang H, Xu Q, et al. Sleep drives metabolite clearance from the adult brain. Science 2013;342:373–377.

See www.StemCellsTM.com for supporting information available online.